





Cite this: *Soft Matter*, 2024, 20, 8937

## Supramolecular chiroptical sensing of chiral species based on circularly polarized luminescence

Panyang Chen,<sup>a</sup> Huahua Fan,<sup>bc</sup> Sifan Du,<sup>c</sup> Xin Wen,<sup>c</sup> Li Zhang \*<sup>c</sup> and Minghua Liu \*<sup>ac</sup>

Circularly polarized luminescence (CPL) refers to the differentiation of the left-handed and right-handed emissions of chiral systems in the excited state. Serving as an alternative characterization method to circular dichroism (CD), CPL can detect changes in fluorescence in a chiral system, which could be more efficient in recognizing chiral species. Although CPL can be generated by attaching luminophores to a chiral unit through a covalent bond, the non-covalent bonding of fluorescent chromophores with chiral species or helical nanostructures can also induce CPL and their changes. Thus, CPL can be used as an alternative detection technique for sensing chiral species. In this review, we summarize typical recent advances in chirality sensing based on CPL. The determination of the absolute configuration of chiral compounds and encrypted sensing is also discussed. We hope to provide useful and powerful insights into the construction of chemical sensors based on CPL.

Received 9th August 2024,  
Accepted 15th October 2024

DOI: 10.1039/d4sm00960f

[rsc.li/soft-matter-journal](http://rsc.li/soft-matter-journal)

### 1. Introduction

Chiral materials with chiroptical properties can absorb or emit circularly polarized light without any waveplates. When the materials prefer to absorb left- or right-handed circularly polarized light, they show circular dichroism (CD). When the materials prefer to emit left- or right-handed circularly polarized light, they show circularly polarized luminescence (CPL).<sup>1,2</sup> Compared with circular dichroism (CD) utilized to characterize structural information in the ground state, CPL can provide excited-state information on chiral luminescent systems and thus could serve as an alternative method to CD. Moreover, CPL offers unique functions related to chiroptical materials in terms of chirality generation, transfer and amplification. The magnitude of CPL is generally quantified using the luminescence dissymmetry factor,  $g_{\text{lum}} = 2(I_{\text{L}} - I_{\text{R}})/(I_{\text{L}} + I_{\text{R}})$ , where  $I_{\text{L}}$  and  $I_{\text{R}}$  are the emission intensities of left- and right-handed circularly polarized light, respectively. In the molecular state,  $g_{\text{lum}}$  values showed positive correlations with  $g_{\text{abs}}$  (obtained from a CD spectrum) in small organic molecule systems, indicating a strong relationship between these two photo-physical processes. However, owing to the intrinsic differences

between excitation and luminescence processes, dissymmetry factors for these two processes can be significantly varied upon interaction with other species.<sup>3–9</sup>

Currently, CPL-active materials have been extensively investigated in various fields of scientific research, such as 3D optical displays, photoelectric devices, asymmetric catalysts, advanced security inks, and sensing.<sup>10–16</sup> Generally speaking, CPL could be generated from the involvement of both luminophore and chiral components.<sup>14,17–21</sup> Early research on CPL materials mainly focused on chiral lanthanide complexes owing to the symmetry-forbidden nature of f-f transition, which results in the remarkable enhancement of the luminescence dissymmetry factor ( $g_{\text{lum}}$ ).<sup>14,17,18</sup> In addition, some studies are based on small emissive molecules or complexes with chiral auxiliaries, but characteristics for specific molecules are usually limited because of the defined molecular structure.<sup>22,23</sup> Another effective approach is to construct supramolecular assemblies *via* the self-assembly of chiral or achiral small molecules, which is proven to effectively enrich the versatility of CPL.<sup>24–27</sup>

In recent years, there has been considerable interest in effectively discriminating molecular chirality in the area of chemical sensing owing to the significance of chiral organic molecules and the importance of recognizing their absolute configuration and chiroptical purity.<sup>28–32</sup> Chiral sensing is defined as distinguishing right-handed and left-handed chirality and/or determining the optical purity of chiral compounds. To date, several spectroscopic techniques have been employed to distinguish chiral compounds, including non-chiral spectral techniques,

<sup>a</sup> Zhengzhou University, Zhengzhou 450000, P. R. China. E-mail: liumh@iccas.ac.cn

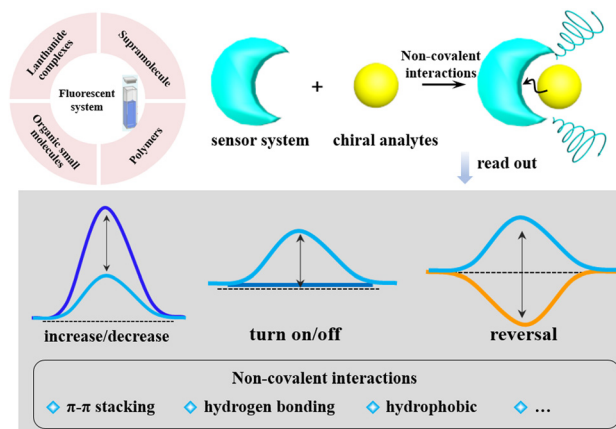
<sup>b</sup> School of Materials Science and Engineering, and Key Lab for Special Functional Materials of Ministry of Education, Henan University, Kaifeng 475004, P. R. China

<sup>c</sup> Key Laboratory of Colloid, Interface and Chemical Thermodynamics, Institute of Chemistry, Chinese Academy of Sciences, Zhongguancun North First Street 2, Beijing, 100190, P. R. China. E-mail: zhangli@iccas.ac.cn

*e.g.*, high-performance liquid chromatography (HPLC), nuclear magnetic resonance (NMR), UV-Vis absorption, fluorescence spectroscopy, and chiroptical techniques, *e.g.*, vibrational circular dichroism (VCD), CD, and CPL.<sup>33–35</sup> CD spectroscopy is mainly employed to characterize biological macromolecules, particularly the tertiary structure of proteins and chiral recognition.<sup>36,37</sup> Nevertheless, many important chiral compounds generate none or only negligible Cotton effects in the UV region due to the lack of a strong chromophore motif, so they are not suitable for characterization by CD spectroscopy. Additionally, the intensity of Cotton effects is closely connected with the extinction coefficient of a chromophore, which directly affects the sensitivity of CD detection limits. In some cases, the absorption of some typical chromophores is lower than 300 nm, and there is an overlap between the substrate absorbance and the introduced chromophore absorbance, which may make it difficult to analyze with the complicated CD spectra.<sup>38,39</sup> The above problems significantly limit the application scope of the CD technique.

However, CPL is a relatively new research field to provide excited-state information on the chiral luminescent system due to the recent availability of commercial instruments. It is expected to exhibit a high signal-to-noise ratio, especially in systems with weak chiral signals or high background noise. The luminescent nature of CPL allows for the detection of weak chirality-induced effects with minimal interference from scattering or solvent contributions, leading to more reliable and accurate chirality sensing results. To design a chiral probe to detect the absolute configuration of chiral analytes, some working principles of the sensing system are expected to be provided. First, the chirality induction or chirality transfer is necessary between the sensor and analytes, or the sensor provides a chiral environment that can induce diastereomeric interactions with the analyte, leading to different binding affinities for the two enantiomers. Second, the sensor system must afford selective recognition sites of molecules that can interact with the analyte, such as hydrogen bonding, ionic interactions, hydrophobic interactions, metal–ligand coordination, and  $\pi$ – $\pi$  stacking. Third, the choice of fluorophores is also important. The luminescent properties could be modulated by the presence of the analyte. Finally, the sensor should be designed to have specificity and sensitivity for the target analyte to minimize interference from other molecules and detect low concentrations of the target enantiomers. Generally, the chiral sensors based on CPL responses consist of modifications of turn on/off, decrease/increase in intensity, and the inversion of the chiral sign. Most reported chiral sensors utilizing CPL signals depend on a turn-on/turn-off signaling mechanism, and other modes are rarely explored.<sup>40–44</sup> Here, this review mainly focuses on chiral sensing based on CPL signals categorized by the components and types of the sensor array (Scheme 1).

For the past few years, CPL spectroscopy has been extensively exploited in many fields of chirality sensing, such as lanthanide complexes, conjugated polymers, supramolecular organic frameworks (SOFs), organic small molecules, and the specifically encrypted sensing of some chiral compounds. It is noteworthy that the highly selective recognition of CPL spectroscopy toward luminescence from chiral assemblies enables us



Scheme 1 Schematic of chiroptical sensing based on circularly polarized luminescence.

to sense target chiral agents or probe molecules, and the chiroptical signal is generated by interactions with chiral assemblies. In particular, a novel type of chiral sensing technique is emerging by utilizing chiral agents or probe molecules to induce CPL signals in microscopic spectroscopy, which can recognize not only the spatial distribution of chiral substances but also their chirality.<sup>45–50</sup> Prompted by the rapid development of chiroptical sensing based on CPL spectroscopy, numerous studies have been conducted on sensing chiral compounds by generating distinct CPL signals, including those of amino acids, nucleotides, proteins, carbohydrates, and other chiral compounds. In this review, we focus on the recent progress of research on chirality sensors based on CPL in the past decade. We mainly summarize the supramolecular chiroptical sensing in the determination of the absolute configuration in different assembled systems and the encrypted sensing of chiral compounds by CPL spectroscopy.

## 2. Determination of the absolute configuration of chiral compounds

Chirality is a property of broken mirror symmetry, and many naturally occurring biological molecules have intrinsic chirality. Chiral molecules are a pair of chiral isomers with opposite handedness and are known as the pair of enantiomers, which exhibit different biochemical behaviors to their mirror-image molecules. For example, proteins are composed of only left-handed amino acids in living organisms, and genetic material DNA is constituted by D-ribose. In addition, more than half of commercial drugs are chiral compounds, and the handedness of enantiomers is significantly concerned with their pharmacology effects and physiological toxicity. In general, single enantiomer drugs are often more effective than their racemic mixtures; more importantly, while one enantiomer constitutes a powerful medicament, the other one may lead to serious side effects; for example, as *R*-thalidomide has a sedative effect in pregnant women while *S*-thalidomide causes severe phocomelia.<sup>51</sup>

Considering this, it is critically important to develop various techniques capable of recognizing and sensing enantiomers that are conducive to eliminating unnecessary side effects in drug development and material sciences. CPL uses the difference in the emission of left- and right-handed circularly polarized light, which is determined by the enantiomer. The sensing of chiral molecules can be achieved by differences in the intensities of the CPL signals generated.

## 2.1. Lanthanide complexes

Lanthanide complexes are known as useful luminescence probe molecules and the earliest to be observed with CPL property owing to their small electrical transition dipole moments and large magnetic transition dipole moments, which endows them with some characteristic properties, such as exceptional and advantageous luminescence properties, high quantum yields, long excited-state lifetimes, and large circularly polarized dissymmetry factors.<sup>22,52</sup> In the meantime, lanthanides play an important role in the field of organic and bioorganic chemistry,<sup>53–57</sup> chemical sensing,<sup>58,59</sup> medicine<sup>60,61</sup> and advanced security inks,<sup>16</sup> and particularly over recent years, chiroptical sensing has been continuously growing. Therefore, lanthanide complexes are outstanding candidates for chirality sensing based on CPL spectroscopy, which are luminescent molecules that generate CPL signals during interactions with target chiral compounds.<sup>24,62–64</sup> Based on these characteristics, lanthanide complexes have been employed for CPL probes, which allows the development of novel chiral probing techniques in microscopic spectroscopy.<sup>65,66</sup>

Iwamura's group proposed a series of achiral  $\text{Eu}^{\text{III}}$  complexes, as shown in Fig. 1, which exhibit detectable CPL signals as a result of the interaction with chiral amino acids, and can be applied for chirality sensing. They first reported a complex  $[\text{Eu}(\text{bda})_2]^-$  (bda = 2,2'-bipyridine-6,6'-dicarboxylic acid) from which induced CPL was generated in the presence of chiral 2-pyrrolidone-5-carboxylic acid, while the test concentration was higher (0.1 M) than that of achiral  $\text{Eu}^{\text{III}}$  complexes ( $1.0 \times 10^{-4}$  M).<sup>67</sup> This result was attributed to the distortion by association with the carboxylate anion of chiral amino acid. To further understand the compatibility of chiral agents and chemical modification of the  $\text{Eu}^{\text{III}}$  probe complexes, the CPL from complex  $[\text{Eu}(\text{pda})_2]^-$  (pda = 1,10-phenanthroline-2,9-dicarboxylic acid) and  $[\text{Eu}(\text{bda})_2]^-$  containing various chiral amino acids were explored.<sup>68</sup>  $[\text{Eu}(\text{pda})_2]^-$  showed intense CPL in the presence of L-histidine or L-arginine ( $g_{\text{lum}} \sim 0.08$ ), while quite weak CPL was observed in the system of  $[\text{Eu}(\text{bda})_2]^-$ , which demonstrated that  $[\text{Eu}(\text{pda})_2]^-$  was good chiral CPL sensing for histidine and arginine in the concentration region of 0.01 M. The authors suggested that the bis(diimine)europium(III) complexes with substituents have rigid ligands that interact with  $-\text{COO}^-$  and  $-\text{NH}_3^+$  groups, which is promising for highly sensitive CPL probe molecules. Another study reported two different europium(III) complexes ( $[\text{Eu}(\text{dppda})_2]^-$  and  $[\text{Eu}(\text{pzpda})_2]^-$ ) with two types of ligands in the chiral sensing system (dppda = 4,7-diphenyl-1,10-phenanthroline-2,9-dicarboxylic acid, pzpda = pyrazino[2,3-f][1,10]phenanthroline-7,10-dicarboxylic acid), and it worked in particular concentration regions (larger than 2 mM).<sup>69</sup> It is worth noting that the CPL signal induced by an amino acid is closely related to the europium (III) complex ligands.

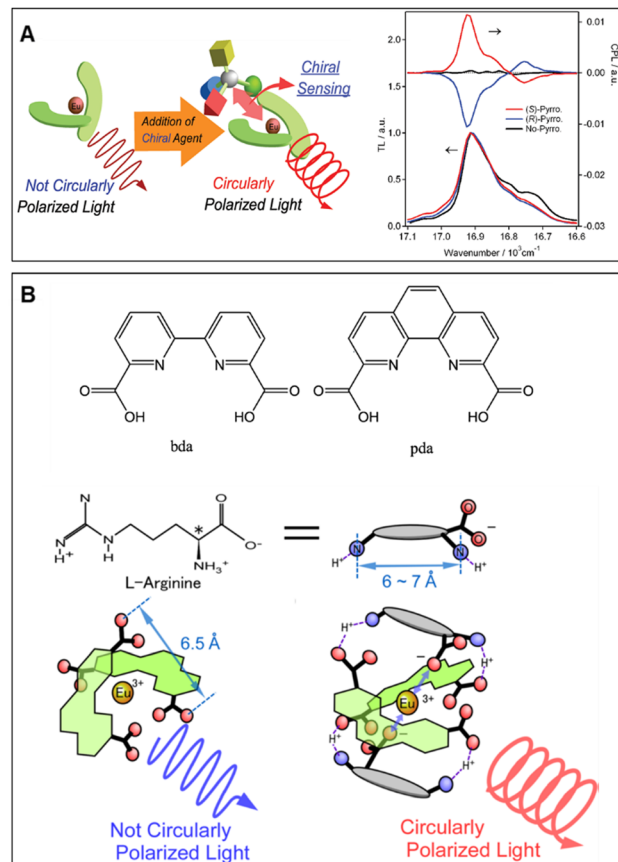


Fig. 1 (A) Chiral sensing using an achiral europium(III) complex induced by circularly polarized luminescence by the chiral agent, reproduced with permission from ACS.<sup>67</sup> (B) Ligands of  $[\text{EuL}_2]^-$ , chiral sensing of amino acids (L-arginine), using induced circularly polarized luminescence of  $[\text{Eu}(\text{pda})_2]^-$ , reproduced with permission from ACS.<sup>68</sup>

For comparison,  $[\text{Eu}(\text{pda})_2]^-$  detected arginine and histidine, while  $[\text{Eu}(\text{dppda})_2]^-$  could achieve selective chiral sensing for chiral ornithine, and  $[\text{Eu}(\text{pzpda})_2]^-$  only recognized histidine, confirming that a chiral-sensing target can be regulated by chemical modification. Additionally, the author investigated the CPL signal of  $[\text{Eu}(\text{pda})_2]^-$  and  $[\text{Eu}(\text{bda})_2]^-$  in mixed aqueous solutions of L- and D-arginine (or histidine).<sup>70</sup> The resulting curves of  $g_{\text{lum}}$  as a function of the D-L mol-fraction revealed that  $[\text{Eu}(\text{pda})_2]^-$  was inclined to form homo-association ( $\text{Eu-pda-L}_2$  or  $\text{Eu-pda-D}_2$ ) instead of hetero-association ( $\text{Eu-pda-L-D}$ ) in the presence of arginine. However, hetero-associated species ( $\text{Eu-pda-L-D}$ ) are dominant in the system containing histidine. These results suggest that the association of a chiral amino acid molecule induces a structural change in  $[\text{Eu}(\text{pda})_2]^-$  to promote chiral selective generation to another molecule (L or D-enantiomer), i.e., homo- or hetero-allosteric association. However, no allosteric-type associations are recognized in the CPL from  $[\text{Eu}(\text{bda})_2]^-$ .

Parker *et al.* reported a europium DO2A-based probe,  $[\text{EuL}_2]^-$ , as shown in Fig. 2A, containing two azaxanthone ligands. It has been studied extensively for selective binding for both alpha-1-acid glycoprotein ( $\alpha_1$ -AGP) and  $\alpha_1$ -antitrypsin ( $\alpha_1$ -AAT) concerning human serum albumin, showing a large induced circularly polarised luminescence (CPL).<sup>71–73</sup> To further systematically

analyze the influence of some deviations for drug binding affinity, another study investigated macrocyclic lanthanide complexes bearing a biaryl chromophore (Fig. 2B),  $[\text{LnL}^1]$ , which exhibits a good affinity for the serum protein  $\alpha_1$ -AGP. A very strong and opposite induced circularly polarized luminescence signal was observed in the presence of human and bovine variants of  $\alpha_1$ -AGP due to the difference in the chiral environment. Moreover, the  $[\text{EuL}^1]$  and  $[\text{TbL}^1]$  complexes could be utilized to monitor the concentration of  $\alpha_1$ -AGP in serum, determining the binding constants of drugs.<sup>74</sup> Adenosine phosphates are of great importance in living organisms. Therefore, their selective recognition and monitoring are promising methods for many biological processes. As natural chiral anions, they can generate a signal detected by chiroptical techniques. As shown in Fig. 2C, europium(III) complexes displayed distinct binding affinities towards  $\text{Zn}^{2+}$  and adenosine phosphates, which consist of an alkynyl-pyridine chromophore with a substituted picolylamine moiety. The resulting studies revealed that strong induced CPL signals of opposite handedness were

obtained in the system of complexes  $[\text{EuL}^3]^+\text{Zn}^{2+}$  and  $[\text{EuL}^4]^+\text{Zn}^{2+}$  upon adding ATP and ADP, thus allowing the ratio of ATP to AMP to be monitored at sub-millimolar/millimolar levels by monitoring the variation of the dissymmetry ratio.<sup>75</sup>

It is quite difficult to detect and recognize simple monosaccharides because of their similar structure. Here, they provide specific spectral patterns of four common monosaccharides *via* CPL induced in europium complexes, which contain ethylenediaminetetraacetic (EDTA) and ethylenetriaminepentaacetic (DEPA) ligands. Meanwhile, the fluorescence decay times confirmed the specific interaction of the spectral response, and it was demonstrated that each sugar may form multiple metal binding modes by combining NMR spectra and molecular dynamics simulations.<sup>76</sup> Additionally, another study was obtained by comparing the CPL spectra of  $\text{Sm}(\text{III})$ ,  $\text{Eu}(\text{III})$  and  $\text{Er}(\text{III})$  ions induced by sialic acid. A strong CPL signal was found in the presence of  $\text{Eu}(\text{III})$  due to the axial conformation of carboxyl and the binding of  $\text{Eu}(\text{III})$  with carboxyl oxygen.<sup>77</sup> It is universally acknowledged that the structure of DNA is easily distorted by sensitizing complexes. Furthermore, few studies of DNA based on CPL spectroscopy have been reported owing to low signal intensity and quenching issues after interaction with sensitizers.<sup>78</sup> At present, the results published by Andrushchenko *et al.*<sup>79</sup> provide the first application for discriminating different DNA structures without the addition of sensitizing agents based on CPL measured using a Raman optical activity (ROA) spectrometer. The ROA/CPL method provides distinct CPL spectra for diverse biomolecules utilizing hydrated  $\text{Eu}(\text{H}_2\text{O})_n^{3+}$  ions, such as deoxyguanosine monophosphate (dGMP) and single- and double-stranded DNA, enabling sensitive sensing of the DNA structure. These results suggest that the ROA/CPL technique is a promising approach for measuring the CPL spectra of complex biomolecules when sensitizers are unavailable.

The properties of the CPL-active material are closely relevant to the luminescent dissymmetry factor and quantum yield. Thus, it is indispensable to obtain a large luminescent dissymmetry factor ( $g_{\text{lum}}$ ) and a high quantum yield to develop desirable CPL materials. To date, the pursuit of large  $g_{\text{lum}}$  value is still very challenging in the CPL research field. Kawai *et al.* successfully fabricated  $D_4$ -symmetrical octanuclear circular  $\text{Ln}^{\text{III}}$  helicates,  $[(R)\text{- or } (S)\text{-}^1\text{Pr-Pybox}]_8(\text{Ln}^{\text{III}})_8(\text{THP})_8$  ( $\text{Ln} = \text{Eu}$  and  $\text{Tb}$ ,  $\text{THP} = \text{tris-}\beta\text{-diketonate}$ ,  $^1\text{Pr-Pybox} = \text{chiral bis}(4\text{-isopropyl-2-oxazolonyl})\text{pyridine}$ ), using a global complexity synthesis strategy.<sup>80</sup> The structural characterization of octanuclear circular  $\text{Ln}^{\text{III}}$  helicates was demonstrated by X-ray crystallographic analysis. Surprisingly, a significant CPL signal with a luminescence dissymmetry factor of 1.25 was observed in circular  $\text{Eu}^{\text{III}}$  helicates, corresponding to  $^5\text{D}_0 \rightarrow ^7\text{F}_1$  transition at 592 nm. It should be noted that visible identification of the difference between left and right circularly polarized emissions of  $R$  and  $S$  isomers could be achieved due to the remarkable  $g_{\text{lum}}$  of the circular  $\text{Eu}^{\text{III}}$  helicate in chloroform and PMMA thin film. The present study further opens up a new direction for CPL visible recognition and significantly extends the application of CPL-active materials to future security printing systems, 3D displays, and chiroptical sensors.

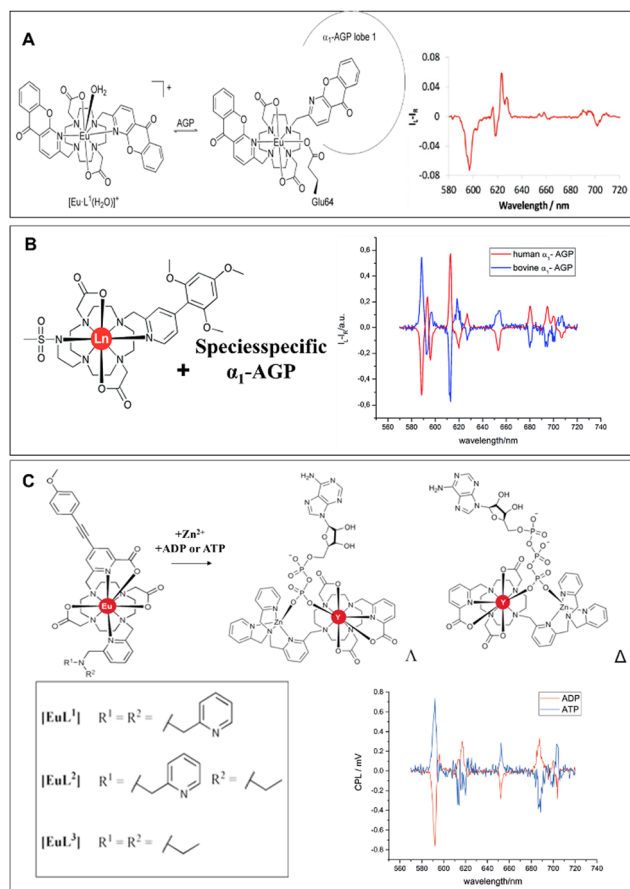


Fig. 2 (A) Reversible binding of the macrocyclic lanthanide complex to  $\alpha_1$ -AGP and CPL spectra of  $[\text{EuL}^1]^+$  in the presence of  $\alpha_1$ -AGP, reproduced with permission from RSC.<sup>71</sup> (B) Molecular structure of lanthanide complexes and induced CPL spectra of  $[\text{EuL}^1]$  in the presence of human and bovine  $\alpha_1$ -AGP, reproduced<sup>73,74</sup> with permission from Wiley-VCH and RSC. (C) Molecular structures of  $[\text{EuL}^1\text{-}3]$ , optimized model geometries and CPL spectra for  $[\text{EuL}^1]^+\text{Zn}^{2+}\text{ADP}$  and  $[\text{EuL}^1]^+\text{Zn}^{2+}\text{ATP}$ , reproduced with permission from Wiley-VCH.<sup>75</sup>

## 2.2. Organic small molecules

Organic small molecules have attracted much attention due to their lower density, lighter weight and attractive chiroptical properties, which play a crucial role in many potential applications. Over the past few decades, CPL spectroscopy based on organic small molecules has received considerable attention owing to the structural properties of their excited states. As shown in Fig. 3A, it has been reported that Schiff base complexes can be formed *in situ* by mixing amino acids or amino alcohols with a commercial 1-hydroxy-2-naphthaldehyde.<sup>81</sup> With the addition of  $\text{Al}^{3+}$ , the fluorescence spectra were significantly enhanced, and obvious CPL signals were observed. Enantioselectivity sensing could be achieved by comparing the intensity and sign of CD and CPL, which can not only be applied to sense the absolute configuration of amino acid and amino alcohol but also accurately quantify enantiomeric excess values by dissymmetry factors of CD and CPL signals.

Kawai and co-workers proposed novel luminescence probes using pyrene derivatives with CPL as signal output.<sup>82</sup> As illustrated in Fig. 3B, chiral molecules (*R,R*)- $\text{Im}_2\text{Py}$  and (*S,S*)- $\text{Im}_2\text{Py}$  are synthesized by linking two chiral imidazole groups at the 1,6-positions of pyrene through ethynyl spacers. Upon tetrahedral coordination with  $\text{Zn}^{2+}$ , probe molecules spontaneously self-assemble into the chiral arrangement of P or M, exhibiting intense CD and CPL signals. It is demonstrated that CPL can be applied for object identification in sensor systems. By comparing the mapping image of photoluminescence (PL:  $I_L + I_R$ ) and circularly polarized luminescence (CPL:  $I_L - I_R$ ), rhodamine 6G with similar luminescence to (*S,S*)- $\text{Im}_2\text{Py}$  was selected as a non-target species to detect differences before and after the addition of probe molecules. It was found that the CPL mapping images showed significant variations between the two regions, while the PL mapping images had no remarkable differences,

enabling us to distinguish different signals from the target analyte and non-target species *via* the CPL technique.

The development of chiral functional materials based on histidine derivatives is deeply inspired by the importance of imidazole-mediated H-bonding interactions in supramolecular assemblies. Liu *et al.* designed and synthesized a series of chiral  $\pi$ -histidine amphiphilic molecules in which the imidazole heading moieties can form directional hydrogen bonds with amide and carboxylic acid groups, thus significantly affecting the nano assembly and chiral properties. On this basis, the author introduced the tetraphenylethylene (TPE) group into  $\pi$ -histidine system because of its aggregation-induced emission properties, reporting such a straightforward strategy for enantioselective recognition and chiral matching in a binary system consisting of luminescent chiral tetraphenylethylene-histidine (TPEHis) and fluorenylmethoxycarbonyl-alanine (FmocAla).<sup>83</sup> It was found that TPEHis and FmocAla with the same chirality (L/L or D/D) could cooperatively co-assemble to form double helical  $\pi$ -aggregates, leading to the significant enhancement of both CPL signal and quantum yield ( $g_{\text{lum}} = 0.14$  and QY = 0.76). However, the co-assembly of TPEHis and FmocAla with opposite chirality (L/D or D/L) exhibited unordered aggregates and led to CPL silence. In addition, the methyl groups of alanine and the Fmoc chromophore are indispensable for the formation of the double helix, revealing the structural complementation of Fmoc-alanine and TPEHis. Simultaneously, single-crystal X-ray crystallography, computational modeling and spectroscopy data also confirmed the result. It was revealed that the boosted QY and  $g_{\text{lum}}$  value were attributed to the hydrogen bond-assisted  $\pi$  stacking of TPE/Fmoc, which could further reduce the non-radiative decay rate of TPE chromophores and promote asymmetric exciton couplings.

Zheng *et al.* designed and synthesized new tetraphenylethylene (TPE) helicates with substituents at the 2,6-positions of the

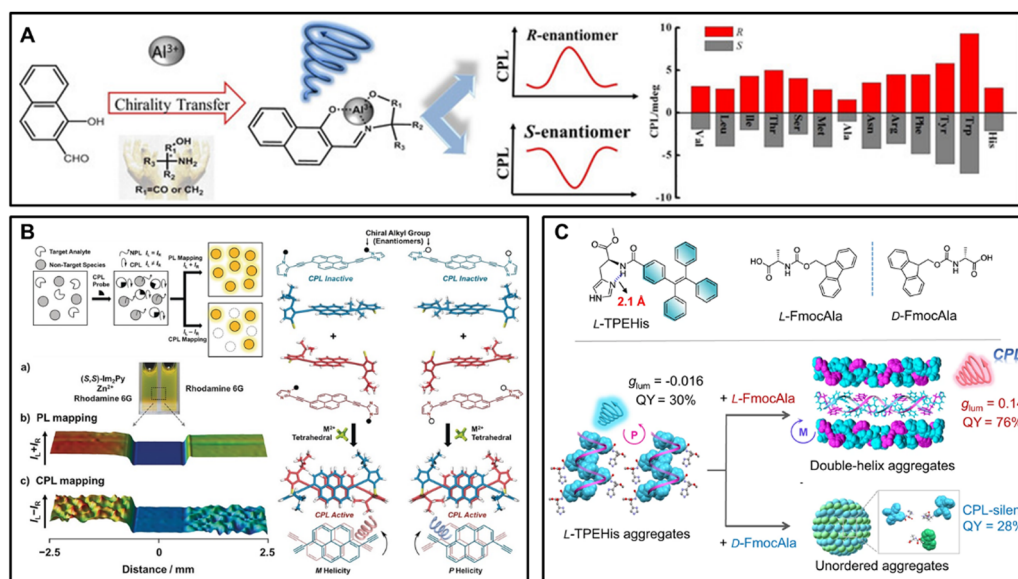
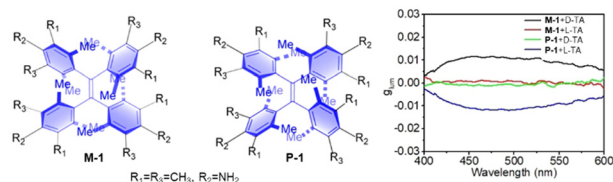


Fig. 3 (A) Chiroptical sensing of amino acids and amino alcohols by *in situ* forming Schiff base complexes in the presence of  $\text{Al}^{3+}$ , reproduced with permission from ACS.<sup>81</sup> (B) Illustration of object identification using CPL signals generated from coordination self-assembly, reproduced with permission from Wiley-VCH.<sup>82</sup> (C) Schematic representation of double helical  $\pi$ -aggregation through enantioselective recognition and chiral matching in a binary system consisting of luminescent chiral L-TPEHis and FmocAla.<sup>83</sup>



Enantioselectivity for chiral recognition of TA and its derivatives by M-1 based on CPL spectra.

Analyte	TA	TA	anTA	tuTA	bzTA
M-1/DSA/TA	1:2:2	1:0:4	1:0:4	1:0:2	1:0:2
$I_D/I_L$	13.9	10.6	35.5	26	204

Fig. 4 Molecular structure of hindered TPE helicites and the change in  $g_{lum}$ , reproduced with permission from Wiley-VCH.<sup>84</sup>

phenyl rings.<sup>84</sup> Interaction with enantiomers of tartaric acid (TA) results in significant CPL enhancement by one TA enantiomer, while the other barely affects CPL signals, highlighting the chiral recognition ability of these helical molecules. Specifically, *D*-TA elicited strong CPL signals for M-6b, while *L*-TA resulted in almost negligible signals for M-6b. The effect of TA enantiomers on M-6b was opposite to that of P-6b. The CPL intensity ratio ( $I_D$ -TA/ $I_L$ -TA) for M-6b evoked by the two TA enantiomers reached 10.6. 6b helicite also exhibited enantioselectivity toward other TA derivatives, such as di-*p*-anisoyl-tartaric acid (anTA), dibenzoyl-tartaric acid (bzTA), and ditoluoyl-tartaric acid (tuTA). The CPL intensity ratios ( $I_D$ -TA/ $I_L$ -TA) for M-6b evoked by the two enantiomers of anTA, tuTA, and bzTA were 35.5, 26, and 204, respectively (Fig. 4).<sup>85</sup>

### 2.3. Conjugated polymer

Conjugated polymer is an important class of organic material with a large number of conjugated repeat units that have excellent optical performance and multifunctional chemical structure. It has been used extensively for sensing amino acids, and the ability of chiral recognition can be enhanced by regulating the structure of conjugated polymers, thus improving the sensitivity of detection. To date, although polymer-based chemical sensing has been reported,<sup>86</sup> there has been no report on polymer-based CPL sensors. In comparison with organic small molecules, the enhancement of the chiroptical signal can be achieved in the achiral-conjugated polymer by the induction of chiral molecules. Fig. 5A shows an achiral Eu(III)-containing conjugated polymer, designed and synthesized by Cheng's group.<sup>11</sup> It was found that no CPL was observed in the solution of P3 and the model molecule. Upon the addition of proline, intense CPL was obtained. Interestingly, a higher optical anisotropy factor could be detected for  $^5D_0 \rightarrow ^7F_1$  at 596 nm in the system of P3 (0.41 for *L*-proline versus  $-0.42$  for *D*-proline). For the model molecule, a  $g_{lum}$  value of  $+0.028$  was obtained in the presence of *L*-proline versus  $-0.036$  for *D*-proline. Additionally, for the  $^5D_0 \rightarrow ^7F_2$  transition at 615 nm, the CPL spectra of P3 also provided a low  $g_{lum}$  value of  $-0.0055$  for *L*-proline while  $g_{lum} = +0.0056$  for *D*-proline. Nevertheless,

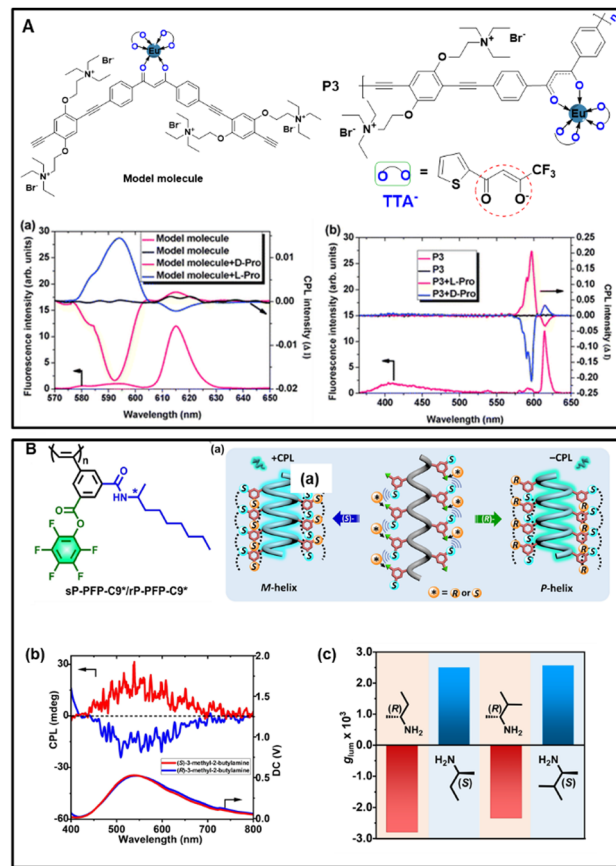


Fig. 5 (A) Molecular structure of the Eu(III)-containing polymer P3, the corresponding model molecule and CPL spectra of the model molecule and P3 in the presence and absence of *L*- and *D*-proline, reproduced with the permission from RSC.<sup>11</sup> (B) Chemical structures of sP-PFP-C9\*/rP-PFP-C9\* and (a) illustration on enantioselective CPL recognition. (b) CPL spectra of sP-PFP-C9\* with the addition of (*R*)-/(*S*)-3-methyl-2-butylamine. (c) CPL responses of sP-PFP-C9\* towards various chiral amines after reaction for 24 h, reproduced with permission from Wiley-VCH.<sup>87</sup>

the  $g_{lum}$  value of the model molecule was less than 0.001. The results indicate that P3 exhibits preferable sensitivity to proline due to the specific guest-molecule orientation of the conjugated polymer. This research revealed that the chiral amino acid could induce the amplification effect of the CPL signal in the conjugated polymer and afford a new method to obtain a higher optical anisotropy factor for CPL-active polymer materials.

Wan's group reported a novel self-reporting activated ester-amine reaction that offers multi-channel visual detection of organic amines.<sup>87</sup> The polymers bearing an achiral pentafluorophenol (PFP) activated ester were synthesized. As shown in Fig. 5B, in the presence of an organic amine, an activated ester-amine reaction occurred and consequently triggered the *cis*-transoid to *cis*-cisoid helical transition of the polyphenylacetylene backbone. This transition evokes fluorescence, providing a visible readout for the detection of organic amines. Furthermore, due to the existence of helicity and photoluminescence, CPL was anticipated as the ultimate product. These products could potentially serve as enantioselective CPL detectors, facilitating the determination of the configuration and enantiomeric excess

(ee) values of chiral amines. In the cases of 2-butylamine and 3-methyl-2-butylamine, the polymer solution displayed positive CPL signals for (*S*)-enantiomers and negative signals for (*R*)-enantiomers, indicating that the chirality of the amines dictated the screw sense of the final products. By leveraging this enantioselective CPL recognition, we determined the enantiomeric excess (ee) value of 3-methyl-2-butylamine. As the content of the (*R*)-enantiomer increased, absorption signals around 350 nm gradually shifted from negative to positive values. Similar conclusions were drawn from the chiral excited state spectra. Notably, the solution exhibited a large negative CPL signal at high contents of the (*R*)-enantiomer (0–100 ee%). Upon reducing the content of the (*R*)-enantiomer, the CPL signal gradually shifted towards positive values, reaching a maximum positive value at an ee of approximately 90%. Thus, the enantiomeric composition could be accurately determined from the CPL signal across a wide variation range, showing the potential of this polymer as an enantioselective CPL detector.

#### 2.4. Supramolecular organic framework

In recent years, chiral framework materials are a class of emergent chiral materials that have been applied in many fields, including chiral separation, asymmetric catalysis, and chiral sensing.<sup>88–96</sup> It has been rapidly developed due to their unique structural characteristics, such as their highly regular structure, permanent porosity, and asymmetric interspace. Some typical chiral framework materials include chiral zeolitic imidazolate frameworks (ZIFs), metal organic frameworks (MOFs), covalent organic frameworks (COFs), and supramolecular organic frameworks (SOFs). Hereinto, SOFs are constructed *via* non-covalent interactions. Cao *et al.* report and synthesize an achiral cucurbit[8]uril-based SOF (SOF-1) with adaptive chirality, which is formed from cucurbit[8]uril and tetra(6-coumarinylmethyl-pyridinium)tetraphenylethylene derivative *via* host-guest complexation.<sup>97</sup> In the meantime, mirror-image CD ( $g_{\text{abs}} \approx \pm 10^{-4}$ ) and CPL ( $g_{\text{lum}} \approx \pm 10^{-4}$ ) signals were induced in the presence of phenylalanine through efficient through-space chirality transfer, M-SOF-1 induced by *L*-Phe and P-SOF-1 induced by *D*-Phe (Fig. 6). More interestingly, a small amount of ATP or ADP (0.4 equiv.) could also successfully induce the generation of chiral signals *via* electrostatic interactions. Moreover, based on the characteristic CD spectra of SOF  $\supset$  peptides, Phe-Ala and Phe-Phe could be distinguished from di- and tripeptides, and distinct CD signals were obtained at 323–470 nm. Furthermore, the adaptive chirality of SOF-1 can be applied to distinguish their sequences for Phe-Ala ( $g_{\text{abs}} = -4.1 \times 10^{-5}$ ) and Ala-Phe (ND) and some polypeptides/protein (*e.g.*, somatostatin and human insulin) with characteristic CD spectra.

### 3. Encrypted sensing on biomolecules

Sometimes, specific recognition cannot be achieved by exploiting conventional techniques, such as fluorescence and CD. Therefore, it is urgent to develop a new technology for encrypted sensing to achieve selectively recognize chiral analytes. Recently, considerable interest has focused on stimuli-responsive chiroptical functional materials with CPL. In

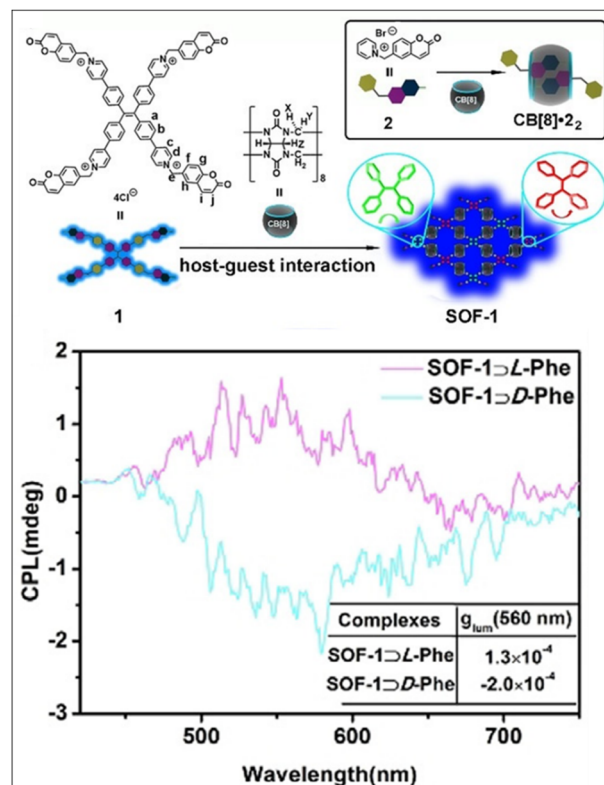


Fig. 6 Adaptive chirality of the achiral cucurbit[8]uril-based supramolecular organic framework (SOF-1) induced by *L*/*D*-phenylalanine, reproduced<sup>90</sup> with permission from Wiley-VCH.<sup>97</sup>

particular, a switchable supramolecular system is endowed with CPL, which can facilitate the construction of multiple information channels to optimize variable performance and enable the encryption of target analytes. Here, Fig. 7A illustrates an example displaying reversible switches of FL and CPL between different molecular configurations.<sup>98</sup> A chiral histidine amphiphile functionalized by styrene-thiazole (abbreviated as STH) could coordinate with alkaline earth metal ions. Interestingly, a disassembly process occurred owing to the *trans*-*cis* isomerization of styrene upon UV irradiation, showing silent FL and CPL signals. The *cis* to *trans* configuration transformation of STH was achieved by heating treatment, producing a high-efficiency ON-OFF FL and CPL switch through alternate UV/heating procedures. Impressively, considerable enhancement in the fluorescence was found upon binding of all the three types of adenosines (ATP, ADP, and AMP) with no significant difference. Nevertheless, the addition of ATP (or ADP) leads to the quenching of the CPL signal in the system of STH/ $\text{Mg}^{2+}$  while strong CPL activity remains only in the presence of AMP, which possesses the efficiently encrypted selective recognition ability of AMP based on CPL. The detection concentration of AMP is around 5 mM.

In recent years, there have been many reports about terpyridine-containing derivatives and their metal complexes due to their outstanding photophysical and electrochemical performance.<sup>100–102</sup> In particular, terpyridine-based  $\text{Zn}^{2+}$  complexes are gaining extensive attention and enormous interest in

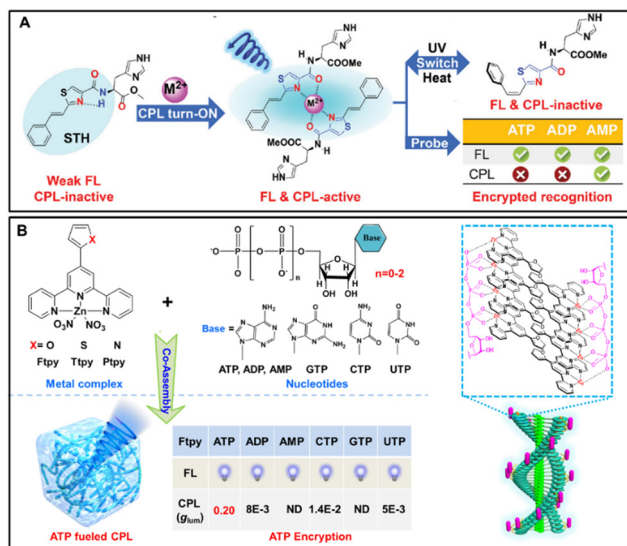


Fig. 7 (A) Molecular structure of L-STH and illustration of the coordination-triggered CPL self-assembly system with an ON-OFF FL and CPL switch and encrypted selective recognition of AMP, reproduced with permission from Wiley-VCH.<sup>98</sup> (B) Molecular structures and co-assembly of achiral terpyridine-Zn(II) complexes and various nucleotides, leading to ATP-induced circularly polarized luminescence (CPL) with a high dissymmetry factor than 0.20, reproduced with the permission from Wiley-VCH.<sup>99</sup>

supramolecular and material chemistry because of synthesis accessibility, rich photophysical properties and excellent coordination affinity.<sup>103–105</sup> ATP, as an important chiral biomolecule, can interact with various small molecules to form chiral assemblies in the field of supramolecular chemistry. Inspired by this progress and the high binding affinity of ATP to metal ions, Liu *et al.* investigated an ATP-driven supramolecular self-assembly system, synthesized a series of achiral terpyridine-Zn(II) complexes (Ftpy, Ttpy, Ptpy), and studied their co-assembly with ATP and analogues nucleotides.<sup>99</sup> In the system of terpyridine-Zn(II) complexes containing furan group, a similar emission band and intensity were obtained, but only in the presence of ATP, a significantly strong CPL could be observed, and its dissymmetry factor ( $g_{lum}$ ) is as high as 0.20, suggesting that the specific recognition and selective interaction of ATP are further achieved by CPL spectra. It is worth noting that although the  $g_{lum}$  value of Ttpy/ATP is lower than that of Ftpy/ATP for the terpyridine-Zn(II) complexes containing the thiophene group, ATP can also be selectively recognized by the generation of a CPL signal. In the system of pyrrole-substituted Zn(II)-terpyridine, no CPL signal was detected. The density functional theory results confirmed that the high CPL signal depended on the planar conformation of Ftpy in the presence of ATP. Considering that the  $g_{lum}$  value of the Ftpy/ATP system is much larger than that of the Ftpy/AMP system, ATPases were added, and the CPL spectra of Ftpy/ATP co-assembly were measured *in situ*. It was found that the CPL signal decreased gradually over time due to enzymatic hydrolysis. Finally, the CPL signal is similar to the Ftpy/AMP, which is speculated to be the conversion of ATP to AMP by enzymatic hydrolysis. This

research opens up a new direction for ATP-encrypted recognition based on CPL and provides the possibility of designing functional materials that simulate natural biological materials.

## 4. Conclusions

In conclusion, CPL-active materials have aroused significant attention because of their potential applications in chiral optical sensors, liquid crystal lasers, chiroptical switches, optical storage devices, and 3D optical displays. Herein, we highlighted the recent progress of CPL-active materials in the field of chiral sensing. By virtue of various building blocks, CPL-active materials with different optical properties can be fabricated, which can selectively sense and recognize various chiral analytes, including chiral amino acids, proteins, nucleotides, carbohydrates and other compounds. Recent advances have been reported concerning chirality sensing based on CPL to classify two categories: determination of the absolute configuration (or enantiomeric excess) of chiral compounds and encrypted sensing. Although the first can detect and analyze the different emissions of left- and right-handed circularly polarized light, which is determined by the handedness of the enantiomer, the latter allows for the encrypted sensing of chiral analytes based on CPL instead of other spectral techniques. We anticipate that the present work will stimulate the development of CPL-active materials and provide a useful and profound understanding of supramolecular chiroptical sensing based on CPL.

Nonetheless, there are still many challenges that remain and further efforts need to be greatly devoted to the field of CPL-active materials. A large luminescent dissymmetry factor ( $g_{lum}$ ) and a high quantum yield, which are key and difficult points to explore and overcome in the future, provide extensive space for its visible recognition and sensing.

## Author contributions

Panyang Chen and Huahua Fan: conceptualization, and writing – original draft preparation. Sifan Du, Xin Wen, Li Zhang, and Minghua Liu: writing – reviewing and editing. Panyang Chen and Huahua Fan contributed equally.

## Data availability

No primary research results, software or code has been included and no new data were generated or analysed as part of this review.

## Conflicts of interest

There are no conflicts to declare.

## Acknowledgements

This research was funded by the National Key Research and Development Program of China (2022YFA1204402).

## Notes and references

- 1 W. Chen, K. Ma, P. Duan, G. Ouyang, X. Zhu, L. Zhang and M. Liu, *Nanoscale*, 2020, **12**, 19497–19515.
- 2 M. Saqlain, H. M. Zohaib, S. Qamar, H. Malik and H. Li, *Coord. Chem. Rev.*, 2024, **501**, 215559.
- 3 P. Wu, A. Pietropaolo, M. Fortino, S. Shimoda, K. Maeda, T. Nishimura, M. Bando, N. Naga and T. Nakano, *Angew. Chem., Int. Ed.*, 2022, **61**, e202210556.
- 4 P. Wu, A. Pietropaolo, M. Fortino, M. Bando, K. Maeda, T. Nishimura, S. Shimoda, H. Sato, N. Naga and T. Nakano, *Angew. Chem., Int. Ed.*, 2023, **62**, e202305747.
- 5 Q. Wang, K. Son, A. Pietropaolo, M. Fortino, M. Ogasawara, T. Ohji, S. Shimoda, M. Bando and T. Nakano, *Chem. – Eur. J.*, 2024, **30**, e202304275.
- 6 Q. Wang, A. Pietropaolo, M. Fortino, Z. Song, M. Bando, N. Naga and T. Nakano, *Chirality*, 2022, **34**, 317–324.
- 7 Z. Zhang, T. Harada, A. Pietropaolo, Y. Wang, Y. Wang, X. Hu, X. He, H. Chen, Z. Song, M. Bando and T. Nakano, *Chem. Commun.*, 2021, **57**, 1794–1797.
- 8 Z. Song, H. Sato, A. Pietropaolo, Q. Wang, S. Shimoda, H. Dai, Y. Imai, H. Toda, T. Harada, Y. Shichibu, K. Konishi, M. Bando, N. Naga and T. Nakano, *Chem. Commun.*, 2022, **58**, 1029–1032.
- 9 M. Bando, M. Fortino, A. Pietropaolo, Y. Shichibu, K. Konishi and T. Nakano, *Chem. Commun.*, 2024, **60**, 8625–8628.
- 10 T. Kawasaki, M. Sato, S. Ishiguro, T. Saito, Y. Morishita, I. Sato, H. Nishino, Y. Inoue and K. Soai, *J. Am. Chem. Soc.*, 2005, **127**, 3274–3275.
- 11 F. Song, G. Wei, X. Jiang, F. Li, C. Zhu and Y. Cheng, *Chem. Commun.*, 2013, **49**, 5772–5774.
- 12 Y. Yang, R. C. da Costa, M. J. Fuchter and A. J. Campbell, *Nat. Photonics*, 2013, **7**, 634–638.
- 13 Y. Yang, R. C. da Costa, D.-M. Smilgies, A. J. Campbell and M. J. Fuchter, *Adv. Mater.*, 2013, **25**, 2624–2628.
- 14 M. C. Heffern, L. M. Matosziuk and T. J. Meade, *Chem. Rev.*, 2014, **114**, 4496–4539.
- 15 C. Hao, R. Gao, Y. Li, L. Xu, M. Sun, C. Xu and H. Kuang, *Angew. Chem., Int. Ed.*, 2019, **58**, 7371–7374.
- 16 L. E. MacKenzie and R. Pal, *Nat. Rev. Chem.*, 2021, **5**, 109–124.
- 17 H. C. Aspinall, *Chem. Rev.*, 2002, **102**, 1807–1850.
- 18 J. C. G. Bunzli and C. Piguet, *Chem. Rev.*, 2002, **102**, 1897–1928.
- 19 Y. Ru, L. Ai, T. Jia, X. Liu, S. Lu, Z. Tang and B. Yang, *Nano Today*, 2020, **34**, 100953.
- 20 Y. Ru, L. Sui, H. Song, X. Liu, Z. Tang, S.-Q. Zang, B. Yang and S. Lu, *Angew. Chem., Int. Ed.*, 2021, **60**, 14091–14099.
- 21 X. Tang, D. Chu, H. Jiang, W. Gong, C. Jiang, Y. Cui and Y. Liu, *Mater. Chem. Front.*, 2020, **4**, 2772–2781.
- 22 S. J. Bradberry, A. J. Savyasachi, M. Martinez-Calvo and T. Gunnlaugsson, *Coord. Chem. Rev.*, 2014, **273**, 226–241.
- 23 J. Roose, A. C. S. Leung, J. Wang, Q. Peng, H. H. Y. Sung, I. D. Williams and B. Z. Tang, *Chem. Sci.*, 2016, **7**, 6106–6114.
- 24 J. A. Kitchen, D. E. Barry, L. Mercks, M. Albrecht, R. D. Peacock and T. Gunnlaugsson, *Angew. Chem., Int. Ed.*, 2012, **51**, 704–708.
- 25 D. Yang, P. Duan, L. Zhang and M. Liu, *Nat. Commun.*, 2017, **8**, 15727.
- 26 H. Zheng, W. Li, W. Li, X. Wang, Z. Tang, S. X.-A. Zhang and Y. Xu, *Adv. Mater.*, 2018, **30**, 201705948.
- 27 C. Gao, Z. Zhang, X. Zhang, J. Chen, Y. Chen, C. Zhao, L. Zhao and L. Feng, *Soft Matter*, 2022, **18**, 3125–3129.
- 28 C. Wolf and K. W. Bentley, *Chem. Soc. Rev.*, 2013, **42**, 5408–5424.
- 29 H. H. Jo, C.-Y. Lin and E. V. Anslyn, *Acc. Chem. Res.*, 2014, **47**, 2212–2221.
- 30 X. Zhang, J. Yin and J. Yoon, *Chem. Rev.*, 2014, **114**, 4918–4959.
- 31 Z. Chen, Q. Wang, X. Wu, Z. Li and Y.-B. Jiang, *Chem. Soc. Rev.*, 2015, **44**, 4249–4263.
- 32 X. Liang, W. Liang, P. Jin, H. Wang, W. Wu and C. Yang, *Chemosensors*, 2021, **9**, 279.
- 33 X. F. Mei and C. Wolf, *J. Am. Chem. Soc.*, 2004, **126**, 14736–14737.
- 34 H. M. Seifert, Y.-B. Jiang and E. V. Anslyn, *Chem. Commun.*, 2014, **50**, 15330–15332.
- 35 K. Staszak, K. Wieszczycka, V. Marturano and B. Tylkowski, *Coord. Chem. Rev.*, 2019, **397**, 76–90.
- 36 S. M. Kelly and N. C. Price, *Curr. Protein Pept. Sci.*, 2000, **1**, 349–384.
- 37 J. Heo and C. A. Mirkin, *Angew. Chem., Int. Ed.*, 2006, **45**, 941–944.
- 38 I. AkritopoulouZanze, K. Nakanishi, H. Stepowska, B. Grzeszczyk, A. Zamojski and N. Berova, *Chirality*, 1997, **9**, 699–712.
- 39 X. F. Huang, K. Nakanishi and N. Berova, *Chirality*, 2000, **12**, 237–255.
- 40 K. Takaishi, C. Maeda and T. Ema, *Chirality*, 2023, **35**, 92–103.
- 41 J. Gong, R. Huang, C. Wang, Z. Zhao, B. Z. Tang and X. Zhang, *Dyes Pigm.*, 2022, **198**, 109969.
- 42 J. Gong and X. Zhang, *Coord. Chem. Rev.*, 2022, **453**, 214329.
- 43 Y. Liu and P. Xing, *Adv. Mater.*, 2023, **35**, e2300968.
- 44 J. Zhao, K. Zeng, T. Jin, W.-T. Dou, H.-B. Yang and L. Xu, *Coord. Chem. Rev.*, 2024, **502**, 215598.
- 45 G. Marriott, M. Heidecker, E. P. Diamandis and Y. Yanmarriott, *Biophys. J.*, 1994, **67**, 957–965.
- 46 G. Vereb, E. Jares-Erijman, P. R. Selvin and T. M. Jovin, *Biophys. J.*, 1998, **74**, 2210–2222.
- 47 K. Claborn, E. Puklin-Faucher, M. Kurimoto, W. Kaminsky and B. Kahr, *J. Am. Chem. Soc.*, 2003, **125**, 14825–14831.
- 48 A. Matsugaki, H. Takechi, H. Monjushiro and H. Watarai, *Anal. Sci.*, 2008, **24**, 297–300.
- 49 K. Mawatari, S. Kubota and T. Kitamori, *Anal. Bioanal. Chem.*, 2008, **391**, 2521–2526.
- 50 H. Tsumatori, T. Nakashima and T. Kawai, *Org. Lett.*, 2010, **12**, 2362–2365.
- 51 T. Ito and H. Handa, *Congenital Anomalies*, 2012, **52**, 1–7.

- 52 J. L. Lunkley, D. Shirotnani, K. Yamanari, S. Kaizaki and G. Muller, *Inorg. Chem.*, 2011, **50**, 12724–12732.
- 53 N. C. Martinez-Gomez, H. N. Vu and E. Skovran, *Inorg. Chem.*, 2016, **55**, 10083–10089.
- 54 S. Chen, D. Yan, M. Xue, Y. Hong, Y. Yao and Q. Shen, *Org. Lett.*, 2017, **19**, 3382–3385.
- 55 H. Pellissier, *Coord. Chem. Rev.*, 2017, **336**, 96–151.
- 56 V. L. Weidner, C. J. Barger, M. Delferro, T. L. Lohr and T. J. Marks, *ACS Catal.*, 2017, **7**, 1244–1247.
- 57 M. Oliverio, M. Nardi, P. Costanzo, M. L. Di Gioia and A. Procopio, *Sustainability*, 2018, **10**, 721.
- 58 X. H. Huang, L. Shi, S. M. Ying, G. Y. Yan, L. H. Liu, Y. Q. Sun and Y. P. Chen, *CrystEngComm*, 2018, **20**, 189–197.
- 59 Y. Zhang, S. Yuan, G. Day, X. Wang, X. Yang and H.-C. Zhou, *Coord. Chem. Rev.*, 2018, **354**, 28–45.
- 60 S. Lacerda and E. Toth, *ChemMedChem*, 2017, **12**, 883–894.
- 61 S. L. Mekuria, K. D. Addisu, H.-Y. Chou, B. Z. Hailemeskel and H.-C. Tsai, *Colloids Surf., B*, 2018, **167**, 54–62.
- 62 G. Bozoklu, C. Gateau, D. Imbert, J. Pecaut, K. Robeyns, Y. Filinchuk, F. Memon, G. Muller and M. Mazzanti, *J. Am. Chem. Soc.*, 2012, **134**, 8372–8375.
- 63 R. Carr, N. H. Evans and D. Parker, *Chem. Soc. Rev.*, 2012, **41**, 7673–7686.
- 64 J. Yuasa, T. Ohno, H. Tsumatori, R. Shiba, H. Kamikubo, M. Kataoka, Y. Hasegawa and T. Kawai, *Chem. Commun.*, 2013, **49**, 4604–4606.
- 65 G. A. Hembury, V. V. Borovkov and Y. Inoue, *Chem. Rev.*, 2008, **108**, 1–73.
- 66 J. Yuasa, T. Ohno, K. Miyata, H. Tsumatori, Y. Hasegawa and T. Kawai, *J. Am. Chem. Soc.*, 2011, **133**, 9892–9902.
- 67 M. Iwamura, Y. Kimura, R. Miyamoto and K. Nozaki, *Inorg. Chem.*, 2012, **51**, 4094–4098.
- 68 K. Okutani, K. Nozaki and M. Iwamura, *Inorg. Chem.*, 2014, **53**, 5527–5537.
- 69 T.-a. Uchida, K. Nozaki and M. Iwamura, *Chem. – Asian J.*, 2016, **11**, 2415–2422.
- 70 M. Iwamura, M. Fujii, A. Yamada, H. Koike and K. Nozaki, *Chem. – Asian J.*, 2019, **14**, 561–567.
- 71 R. Carr, L. Di Bari, S. Lo Piano, D. Parker, R. D. Peacock and J. M. Sanderson, *Dalton Trans.*, 2012, **41**, 13154–13158.
- 72 R. Carr, R. Puckrin, B. K. McMahon, R. Pal, D. Parker and L.-O. Palsson, *Methods Appl. Fluoresc.*, 2014, **2**, 024007.
- 73 L. Jennings, R. S. Waters, R. Pal and D. Parker, *ChemMedChem*, 2017, **12**, 271–277.
- 74 S. Shuvaev, E. A. Suturina, K. Mason and D. Parker, *Chem. Sci.*, 2018, **9**, 2996–3003.
- 75 S. Shuvaev, M. A. Fox and D. Parker, *Angew. Chem., Int. Ed.*, 2018, **57**, 7488–7492.
- 76 T. Wu, J. Prusa, J. Kessler, M. Dracinsky, J. Valenta and P. Bour, *Anal. Chem.*, 2016, **88**, 8878–8885.
- 77 T. Wu and P. Bour, *Chem. Commun.*, 2018, **54**, 1790–1792.
- 78 G. Bobba, J. C. Frias and D. Parker, *Chem. Commun.*, 2002, 890–891.
- 79 T. Wu, P. Bour and V. Andrushchenko, *Sci. Rep.*, 2019, **9**, 1068.
- 80 Y. B. Tan, Y. Okayasu, S. Katao, Y. Nishikawa, F. Asanoma, M. Yamada, J. Yuasa and T. Kawai, *J. Am. Chem. Soc.*, 2020, **142**, 17653–17661.
- 81 Q. Jin, F. Wang, S. Chen, L. Zhou, H. Jiang, L. Zhang and M. Liu, *Chem. – Asian J.*, 2020, **15**, 319–324.
- 82 Y. Imai, Y. Nakano, T. Kawai and J. Yuasa, *Angew. Chem., Int. Ed.*, 2018, **57**, 8973–8978.
- 83 Y. Wang, D. Niu, G. Ouyang and M. Liu, *Nat. Commun.*, 2022, **13**, 1710.
- 84 M. Hu, F. Y. Ye, C. Du, W. Wang, W. Yu, M. Liu and Y. S. Zheng, *Angew. Chem., Int. Ed.*, 2022, **61**, e202115216.
- 85 M. Hu, Y. X. Yuan, W. Wang, D. M. Li, H. C. Zhang, B. X. Wu, M. Liu and Y. S. Zheng, *Nat. Commun.*, 2020, **11**, 161.
- 86 H. Xia, X. Chen, X. Chen, J. Cheng, Y. Liu, X. Chen, Q. Zhang and G. Zou, *Sens. Actuators, B*, 2018, **254**, 44–51.
- 87 S. Wang, S. Xie, H. Zeng, H. Du, J. Zhang and X. Wan, *Angew. Chem., Int. Ed.*, 2022, **61**, e202202268.
- 88 C.-Y. Sun, C. Qin, C.-G. Wang, Z.-M. Su, S. Wang, X.-L. Wang, G.-S. Yang, K.-Z. Shao, Y.-Q. Lan and E.-B. Wang, *Adv. Mater.*, 2011, **23**, 5629–5632.
- 89 M. C. Das, Q. Guo, Y. He, J. Kim, C.-G. Zhao, K. Hong, S. Xiang, Z. Zhang, K. M. Thomas, R. Krishna and B. Chen, *J. Am. Chem. Soc.*, 2012, **134**, 8703–8710.
- 90 P. Wu, C. He, J. Wang, X. Peng, X. Li, Y. An and C. Duan, *J. Am. Chem. Soc.*, 2012, **134**, 14991–14999.
- 91 T. Sawano, N. C. Thacker, Z. Lin, A. R. McIsaac and W. Lin, *J. Am. Chem. Soc.*, 2015, **137**, 12241–12248.
- 92 S. Das, S. Xu, T. Ben and S. Qiu, *Angew. Chem., Int. Ed.*, 2018, **57**, 8629–8633.
- 93 J. Guo, Y. Zhang, Y. Zhu, C. Long, M. Zhao, M. He, X. Zhang, J. Lv, B. Han and Z. Tang, *Angew. Chem., Int. Ed.*, 2018, **57**, 6873–6877.
- 94 X. Chen, H. Jiang, X. Li, B. Hou, W. Gong, X. Wu, X. Han, F. Zheng, Y. Liu, J. Jiang and Y. Cui, *Angew. Chem., Int. Ed.*, 2019, **58**, 14748–14757.
- 95 L. Hu, K. Li, W. Shang, X. Zhu and M. Liu, *Angew. Chem., Int. Ed.*, 2020, **59**, 4953–4958.
- 96 W. Shang, X. Zhu, T. Liang, C. Du, L. Hu, T. Li and M. Liu, *Angew. Chem., Int. Ed.*, 2020, **59**, 12811–12816.
- 97 Y. Li, Q. Li, X. Miao, C. Qin, D. Chu and L. Cao, *Angew. Chem., Int. Ed.*, 2021, **60**, 6744–6751.
- 98 Y. Zhao, D. Niu, J. Tan, Y. Jiang, H. Zhu, G. Ouyang and M. Liu, *Small Methods*, 2020, **4**, 2000493.
- 99 H. Fan, K. Li, T. Tu, X. Zhu, L. Zhang and M. Liu, *Angew. Chem., Int. Ed.*, 2022, e202200727.
- 100 G. Cheng, G. K.-M. So, W.-P. To, Y. Chen, C.-C. Kwok, C. Ma, X. Guan, X. Chang, W.-M. Kwok and C.-M. Che, *Chem. Sci.*, 2015, **6**, 4623–4635.
- 101 S.-Y. Jiao, K. Li, W. Zhang, Y.-H. Liu, Z. Huang and X.-Q. Yu, *Dalton Trans.*, 2015, **44**, 1358–1365.
- 102 D. Chao and S. Ni, *Sci. Rep.*, 2016, **6**, 26477.
- 103 L. J. Liang, X. J. Zhao and C. Z. Huang, *Analyst*, 2012, **137**, 953–958.
- 104 S. Bhowmik, B. N. Ghosh, V. Marjomaki and K. Rissanen, *J. Am. Chem. Soc.*, 2014, **136**, 5543–5546.
- 105 P. Shi, Q. Jiang, X. Zhao, Q. Zhang and Y. Tian, *Dalton Trans.*, 2015, **44**, 8041–8048.